Experimental study of scalar structure in a premixed turbulent methane/air flames

M.S. Boulahlib*

Department of Mechanical Engineering, University Mentouri Constantine (UMC), Algeria.

Abstract

In order to analyze the scalar structure of the premixed flames, an experimental study related to stationary turbulent flames methane-air was carried out. The flames in a Bunsen–type burner, being propagated in a homogeneous and isotropic turbulent flow are stabilized by a pilot flame. This study describes the flame front position and flame brush thickness for various conditions of turbulence and equivalence ratios in the range of Φ=0.6÷1.3. The variation of turbulence intensity and the integral length scale was obtained by means of turbulence grids. The technique of Particles Intercorelated Image Velocimetry (P.I.I.V) was used for the characterization of the isothermal flow field dynamical field of the cold burner. The characterization of the flame front based on the statistical analysis of two-dimensional instantaneous images of the laser sheet tomography (LST) and the fine compensed wire thermometry (F.C.W.T). Contours of flames are extracted from the tomographic recordings and are analyzed by image algorithms to characterize the geometric parameters of the flame during its propagation. The influence of turbulence intensity as well as the equivalence ratio on flame brush thickness was highlighted. The experimental quantification of flame brush starting from the geometrical characteristics of flames front was also obtained.

Keywords: Flame brush thickness; Premixed turbulent combustion; PIIV; LST; FCWT

1. Introduction

The knowledge of the flame structure has to go through a better comprehension of the flow turbulence phenomena and combustion. So, it is necessary to understand the physical and chemical processes dominating within the combustion system. This paper presents experimental results concerning the scalar structure of the stationary premixed turbulent flames located in flamelet regime, in order to characterize the average interaction between the flame scalar field and dynamic one in which it is propagated. In this regime where one assumes a chemical reaction time lower to the turbulence time scale, the effects of the interaction between the phenomena of turbulence and combustion are represented at the same time by the local and global structure of the flame.

The flame is folded by the turbulent flow, which leads to an increase in its surface. Simultaneously, the local structure of the flame is modified by the flame front orientation and shearing of the turbulent flow represented by the flow divergence in the tangent plan flame. Poinsot & al., [1991], based on numerical results obtained from DNS, estimate in the flamelet regime that the small structures able to penetrate and of modify the internal structure of the flame front. Peters [1999], supposes that the small structures can penetrate preheating zone, but which they are unable to disturb the fine reaction zone inside flame front. Lipatnikov & Chomiak [2002], in an article making state of the art, related to the scalar and dynamic structures of premixed turbulent flames, consider that the flame average thickness cannot be only reduced to the validation of numerical models. It seems a characteristic of the turbulent premixed flames as important as turbulent flames speed. Like, the complete comprehension of the physical phenomena and the prediction of a particular lean flame structure with turbulence always remain on update.

* Corresponding author. Tel: 213 793220548;
Fax: 213 318187702; Email: boulahlib@coria.fr

Flame thickness δ_T is the most valuable quantity of the variation of all the medium physical properties of the medium such as the temperature or the concentration of the species, it is regarded as one of the most important spatial characteristics of the premixed turbulent flames. It is used for the normalization of the progress variable evolutions, through flame front to become universal (figure 8).
Many authors have studied the thickness of flame and its interactions with turbulence, chemistry, but the results which exist in the literature remain very few. Karlovitz & al., [1951] had noted that the increase in δ_T was mainly controlled by a law of turbulent diffusion. The first studies are those of Namazian & al., [1987] on V flames.
For Peters [1987] the turbulent thickness of a premixed flame is an important scale characteristic in combustion diagram. By using the laser technique of tomography, Goix [1987] determined turbulent thickness evolution and the its standard deviation for V flames.
Using the Rayleigh Scattering, Boukhalfa [1988], Boukhalfa & al.,[1988a and 1988b], have determined the turbulent thickness and showed that these flames have a very high normalized thicknesses and very close. Deschamps [1990] by examining in a more advanced study of the flames and by using the Rayleigh diffusion coupled with the laser tomography, will confirm work of Boukhalfa [1988], while extending the turbulent intensity range. Y.C. Chen & al., [1996] and A.Buschmann & al, [1996] in their work on premixed turbulent flames scalar structure of methane-air instantaneous and average, are shown the correlation between turbulence, the equivalence ratio and the thicknesses of flames by using the diffusion Rayleigh 2d and the Rayleigh-LIF/OH diffusion. A detailed study of modeling will be carried out by R.O.S. Prasad & al., [1999], and will compare various models of combustion and turbulence with the results of Y.C. Chen & al, [1996]. The results of this comparison, shown an agreement between modeling and the experiment. The flame front position are also of prime importance for the combustor design [KNC Bray 1996 et D. Bradley 1992]. In particular a better understanding of the effects of pressure and turbulence on S_T et δ_T is needed [Griebel 2007].
In a study, A.N.Lipatnikov & J.Chomiak [2002] presents a synthesis on the scalar structure of premixed turbulent flames based on the results of many authors on conical, V and stagnation or spherical flames. L.P.H de Goey & al., [2005] in an experimental, theoretical and numerical study on the instantaneous thickness of the turbulent flames, present measurements carried out by simultaneous images Rayleigh and OH in the flame section. The author highlights the interactions between the structures of turbulence and the crumpling of front flame. The range of the Karlovitz number used moderate remainder. Y.C. Chen & Bilger [2005] measure molar fraction OH, of the scalar structure of the local front, the progress variable and its three-dimensional gradient in a premixed turbulent stagnation flame. Interactions between the various scales of turbulence and the behavior of internal flame front structure are highlighted. Structural transitions of regimes are observed in a relation with the Karlovitz number. S.A.Filatyev & al, [2005] in a series of measurements of premixed turbulent flames properties and in order to validate the models, have presented results on the thickness of the instantaneous reaction zone obtained starting from simultaneous measurements PLIF CH/PIV.
This experimental study shows the small change in the behavior thickness of the flame front against the important variations of turbulence intensity.
A theoretical study on the development of the premixed turbulent flame is presented by A. Lipatnikov & J. Chomiak [2005]. Profiles of progress variable, as well as the development of the flame brush thickness in non stationary flames are presented. A formula for the evaluation of the flame brush thickness is proposed.
Recent measurements of Griebel et al., [2007] were performed in a generic high pressure methane combustor up to 3 MPa. The effects of operating conditions and turbulence on flame front position, turbulent flame and flame brush thickness of lean premixed methane flame at high pressure are investigated experimentally.
In this study, the stationary flames are produced in a turbulent flow, homogeneous and isotropic. The simultaneous effect of several scales of turbulent flow on flames front were studied. Stationary flames were recorded and treated to describe the space properties for various turbulence conditions and equivalence ratios.
In this work the flame characteristics were measured at ambient pressure and temperature, equivalence ratio in the range of Φ=0.6÷1.3, and for inlet bulk velocity of u_{bulk}= 6 m/s. The turbulence intensity and integral length scale at combustor inlet were varied by means of turbulence grids with different geometry. The position and fluctuation of the flame front are characterized by statistical analysis of LST images and FCWT thermometry and their dependence on equivalence ratios, turbulence, Damkohler and Karlovitz numbers are discussed. The flame brush thickness issues from the LST and FCWT techniques are presented and compared.

2. Experimental set up and Post Processing

The used experimental device consists of turbulent Bunsen type burner where the premixing to combustible/air is convected with a mean velocity of 6 m/s (Boulahlib & al., 2004). It contains an annular pilot flame to maintain the flame stabilization resulting from the mixture to

methane/air (equivalence ratio = 0.6 ÷ 1.3). The burner includes a pure feeding system of methane (G20) which is injected radialy into a premixer with seeded air. A laminarisation system of methane-air, and a set of turbulence grids (defined by the hole diameter d and the blockage ratio σ) allows the control of the turbulence level (turbulence intensity and the integral length scale). Spaces between the holes give rise to wakes which mix downstream from the grid. Three perforated plates with hexagonally located holes (18.5, 26.5 and 37.5%) were used (Table 1). In the absence of turbulence grid, the outgoing flow of the burner on a level of very weak turbulence (lower than 1%). The burner exit section has a diameter of 30 mm. The reactive flow is surrounded by an annular air flow having same speed to avoid shearing between burned gases and the surrounding air. The diameter of this coflow is 115 mm, and annular space is 36.5 mm. The grid turbulence is well-known and it is the only one which is connected with a homogeneous and isotropic turbulence. Turbulence is generated by perforated plates located close to the burner exit, where the holes are laid out with a hexagonal grid. This configuration corresponds to the burner rotational symmetry. Interchangeable turbulence can generate various conditions of homogeneous and isotropic turbulence: laminar case and turbulence intensity of 6%, 6.4% and 7.5%. Thus, the flames produced with various conditions of equivalence ratio and turbulence are propagated in the combustion chamber under atmospheric pressure (Figure 1). The characteristics of the turbulent flow like velocities (U and V), there fluctuations (u' and v') and the integral scales (L_{LU}) were determined by Particle Intercorelated Image Velocimetry (E.Rouland [1994]). Table1, summarizes the turbulence characteristics and combustion parameters for the various flames displayed. The ratio u'/S_L, where S_L represents the speed of non-stretched laminar flame, allows to combine the turbulence and combustion conditions. The values of u'/SL vary from 0.83 to 4.25. The studied flames are located in the flamelet regime, except for a lean flame (M0.6), which a Karlovitz number larger than 1.

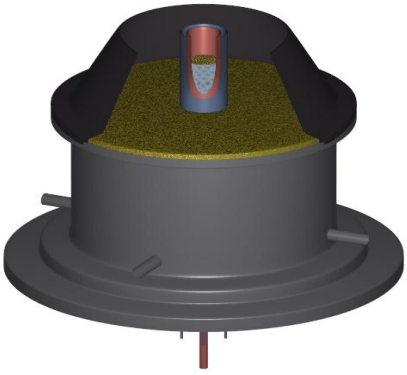

Fig. 1. Burner

2.1 OPTICAL DIAGNOSTICS

The study of the front flames corresponding to the spatial properties requires optical techniques diagnostics and advanced image processing able to follow and describe the combustion process evolution. Instantaneous 2-dimensional visualizations of flames front are obtained by tomography (LST). The use of a laser and a camera let this method well adapted to the turbulent combustion phenomena. It is then possible to visualize the front flames structure and to observe their developments for the various conditions of equivalence ratio and turbulence. Figure 2 shows the arrangements used to produce the laser sheet. The measuring equipment consists of a light source type Laser Nd-Yag 200 mJ Big Sky Laser CFR 200, with a crystal generating a second harmonic, of Q-Switched Laser at the exit with a wavelength 532 Nm. The Laser sheet is obtained by combination of two spherico-cylindrical lenses, thickness about 300 nm. One or two successive images of the section test is recorded using a camera CCD LAVISION FLOW MASTER 3 type fast/double shutter, with a matrix CCD of 1024x1280 pixels. This one is provided with an optics large visible angle Nikkor 50 mm (f:1/1.3). An interferential colored filter centered over the laser wavelength (532 nm) makes it possible to avoid the noise generated by the flame and the various surrounding sources. An electronic system synchronizes the laser with the camera. The flow is seeded with fine olive oil particles (approximately 3 µm), which are evaporated at the entry of the reaction zone, thus creating an important luminous contrast between fresh and burned gases (figure 3a).

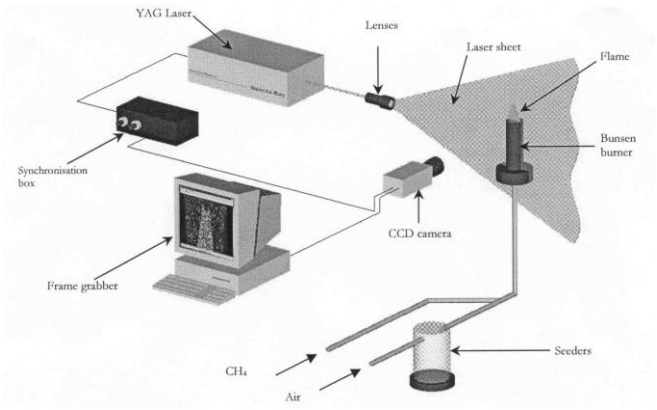

Fig.2. Experimental device

Grid	M(mm)	d(mm)	d/M	σ(%)	C_D (%)
P	2.40	2	0.83	0.38	37.5
M	3.52	3	0.85	0.34	26.5
G	4.54	4	0.88	0.30	18.4

Table 1: *Grids characteristics*

2.1.1. IMAGE TRAITEMENT

In order to extract qualitative information, each flame, is decomposed up into three zones, corresponding to the various stages of its development (figur3a). Spatial resolution of the display system in the two directions is of 70.92 pixel/mm. This allows following precisely the local displacement of flame front. The observed field is of 18x15 cm^2. On each recorded image (figure 3b), a low-pass filter is applied to reduce the background noises and to correct the non-uniformity of the laser sheet. In the presence of flame, the probability density function of the levels of gray presents two peaks corresponding to the area of fresh and burned gases (figure 3c). By choosing a threshold value corresponding to the minimum between the two principal peaks of intensity, the image is binarised. By examining each pixel of this new image, a contour detection algorithm takes into account closest the pixels which delimit the two zones (black and white) defined by the threshold value (figur3d). Contours of flames extracted are then smoothed. This noise comes simultaneously from the digital format for images storage and the used discrete character of seeding. A interpolation treatment is applied on the contour points determined after smoothing. It determines in a very good approximation the polynomial, on each point's interval of the contour, (Renou & al., [2000]) (figure 4). The laser sheet tomography allowed temporal follow-up of reaction zone topological sizes, instantaneous and average contours (Boyer [1980]).

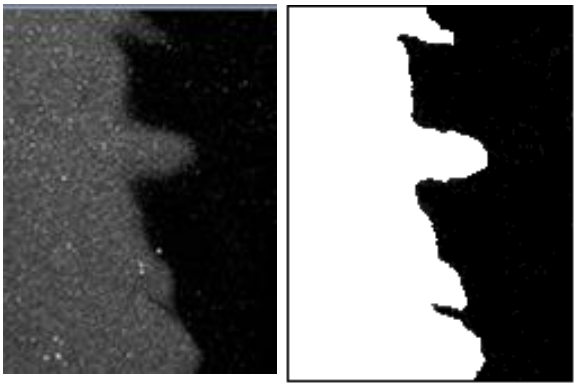

(a) (b)

Fig.3. Mean image obtained by LST (laser sheet tomography), of flame P0.6 (grid P and a equivalence ratio of 0.6). An enlargement of a part of the flame showing a rectangular section of 18x15 cm^2. (b) image after digital processing. White color indicating the unburned and black burned zone.

Using tomographic images, the average sizes of premixed turbulent combustion such as the reaction progress variable, are then obtained from the evolution of the flame front average scalar characteristics. Flame brush thickness in turbulent flow can be defined by the variation of the faces flame instantaneous positions with respect to an average one (R.Said [1989]), starting from the progress variable <c> **,** it is defined as the distance for which <c> is included between 0.1 and 0.9 (Gagnepain [1998] and Pave [2002]), or starting from the expression of Spalding [1955] based on the maximum gradient temperature where it represents the thickness of heat release zone (Namazian & al., [1986], Boukhalfa & al., [1988] and Soika & al., [1998]).

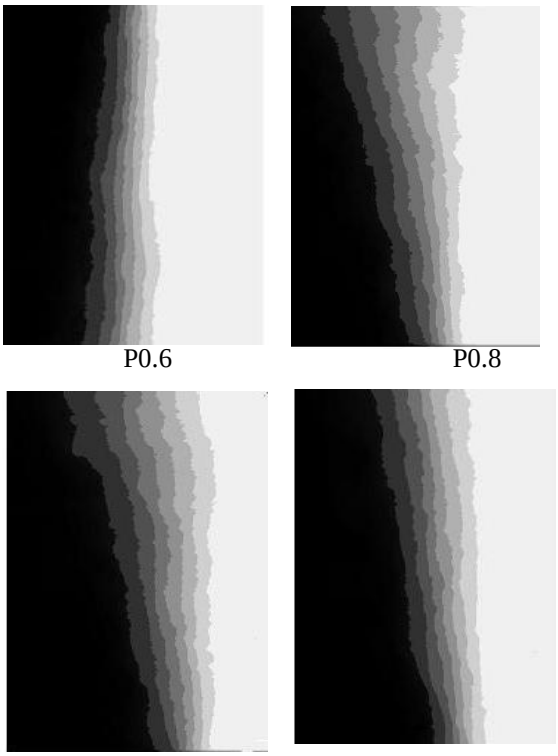

P0.6 P0.8

P0.9 P1.2

Fig. 4: Images of the mean progress variable <c>

2.2 Thermometry set up and Post Processing

The techniques for measuring the flames temperature fall into two categories: intrusive and non-intrusive technique. In our study, the measurement technique by B type thermocouple - FWCT (Fine Wire Compensated Thermocouples) - has been used. This technique is very sensitive to the conditions of temperature and flow velocity. These temperature conditions (velocity and chemical composition of the flow) can affect the physical characteristics of thermocouple materials hence the catalytic effect.

In this study thermocouple type B was used, figure 1 shows this type of thermocouple. The weld heat of these thermocouples is realized between two wires of small-diameter (10 ÷ 500 μ m) to increase the temporal and spatial resolution of the measurement. The wires are fixed to pins more resistant to flow. Each pin is made of the same alloy as the corresponding part of the wire. When

the temperature of the environment is high, the radiant loss becomes important, thus the temperature measured by the hot junction is less than the environment temperature. These losses have been estimated and discussed by many authors, (Paranthoën & Lecordier, [1996], Larras [2000], Ikegami & al. [2003], Moss & al., [2007] and Boulahlib et al., [2008].. Their estimates by one model, can correct the difference between thermocouple temperature and real gas temperature. In addition to that, the temporal resolution of the signal thermocouple is a very important parameter for turbulent flow study. The use of this technique requires an accurate knowledge of heat transfer between the thermocouple and the flow, the physical characteristics of the probe materials, and its geometrical dimensions. That compensation is needed for two reasons: The first relates to the temperature displayed by a thermocouple, which is not necessarily the environment gas temperature, as a result of radiation losses from high temperature thermocouples. For the gas temperature, it is necessary to estimate and correct those losses. The second reason relates to the time response of the thermocouple, which is limited by the inertia of two wires. The digital compensation is then used.

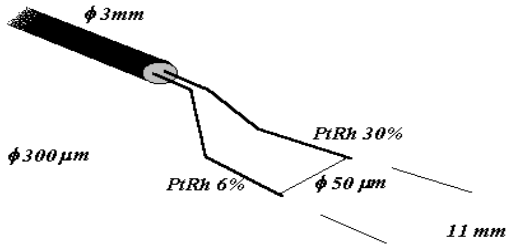

Fig.5. Thermocouple used

Knowing the time response characteristic of the thermocouple, ie time constants τ, we can reconstruct the original temperature signal. The method, which takes into account the convective and radiative effects, is directly extracted from the energy balance. It is determined by introducing the gas temperature and the convective time constant.

The equation can be obtained simultaneously offsetting radiation losses and inertia. This equation is mainly a function of temperature measured by the wire and the Nusselt number. The compensation of inertia thermocouple requires an iterative process. The equation can be obtained simultaneously offsetting radiation losses and inertia. This equation is mainly a function of temperature measured by the wire and the Nusselt number.

The compensation of inertia thermocouple requires an iterative process. The B type thermocouple (Pt30% Rh-Rh Pt6%) is used in the temperature range from 700 to 2000 K, where it owns good signal amplitude (about 9 µ v / K).

A diameter of 50 µ m was chosen to be a good compromise between a low-inertia thermocouple

$$\frac{\partial T_c}{\partial t} = \frac{4Nu\lambda_g}{d^2\rho c_p}\left(T_g(t) - T_c(t)\right) \quad (1)$$

$$\tau_{cv} = \frac{d^2\rho c_p}{4Nu\lambda_g} \quad (2)$$

$$T_g = T_c + \tau_{cv}\left(\frac{\partial T_c}{\partial t} - \frac{\varepsilon_c\varepsilon_{pa}}{1-(1-\varepsilon_c)\cdot(1-\varepsilon_{pa})}\cdot\frac{4\sigma\left(T_c^4 - T_{pa}^4\right)}{d\rho c_p}\right) \quad (3)$$

and sufficient mechanical strength. The theoretical values for uncoated thermocouples were calculated from equations proposed in the literature. The temperature profile is used to define the flame brush thickness δ_T which is defined as the distance between the maximum and the upstream axial location where the level equals 10% of the centerline maximum. This definition is similar to the one proposed by Karpov and Severin [19] and Griebel [13]. They defined the flame brush thickness as the distance between the flame front leading edge and the surface of the ‘‘half-burning’’ which corresponds to the progress variable <C> = 0.5.

3. RESULTS

3.1 turbulence characterization

To determine the characteristics of the turbulence generated by the perforated plates we have made measurements of the mean velocities and fluctuations in non reactive case by P.I.V. G. On the figure 5d, they are represented the evolutions of U^2/u'^2 on the axis adimensioned by the mesh of the holes (Z/M), this allows to determine the decreasing turbulence law coefficients grid still present on the outlet side of the tube.

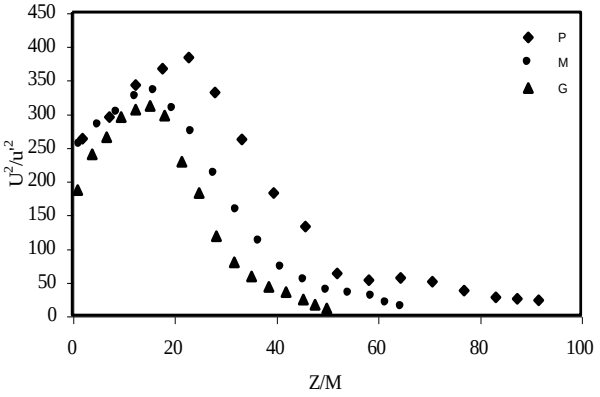

Fig. 6. Radial profiles velocity normalized by u'.

From the fields velocity obtained by P.I.V, and by the application of a rotational operator speed, one can then calculate a macro-scale length, L_{lu}, (figure 6c). We notice fast and linear growth space macro-scales in the potential zone. Then, higher in the jet L_{lu} increases very slightly. Moreover, the values of

the latter are more important for the plates generating an intensity of appreciable turbulence (plate P).

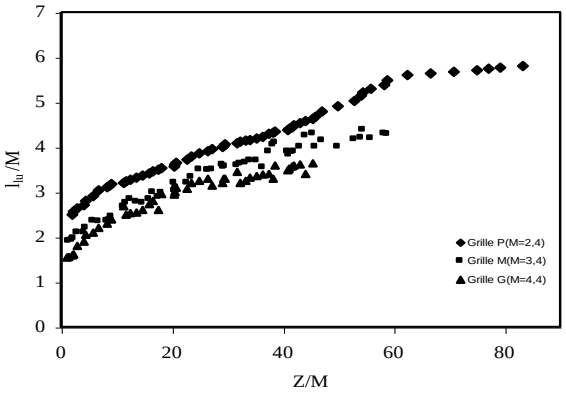

Fig. 7. Length scale L_{lu} on the axis and for the various grids.

3.2 Temperature results

In unburned gas, fluctuations have low values. On average, they are in the range of 20 °C, ie 1.3% of the temperature of the hot gas. In areas of interaction of unburned gas with the combustion zone, one can notice that fluctuations is the highest, they are between 285 and 410 ° C (Figure 2). The results obtained using compensation were very consistent. In this figure, it is clear that the compensation of a digital signal temperature tends to accentuate the gap 1000°C. It would therefore be interesting to interpret the spatial structure characteristic fluctuations depending on their operating conditions [Boulahlib et al., 2008]

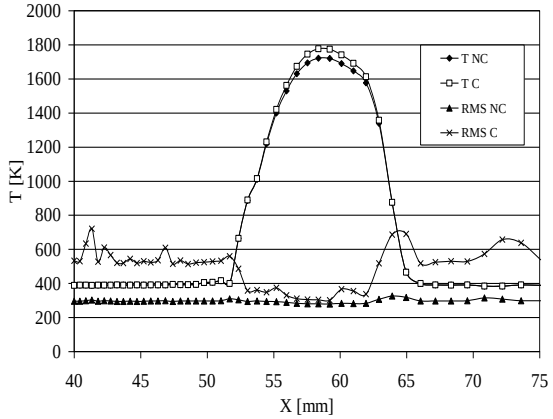

Fig. 8. Profile of temperature and RMS
(C: Compensed and N.C not compensed).

In figure 9, a validation of measurements made by the technique of FWCT was carried out by making a comparison with the methods of optical measurements (Rayleigh Scattering) was carried out. obtained by Boukhalfa [1988]. This comparison shows a good agreement.

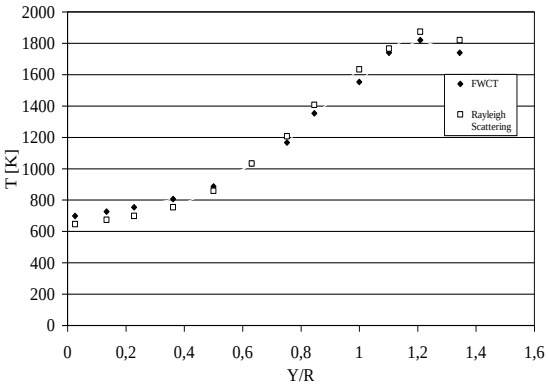

Fig. 9. Comparison of temperature measurement with FWCT and Rayleigh Scattering

3.3 Scalar structure of the flame front

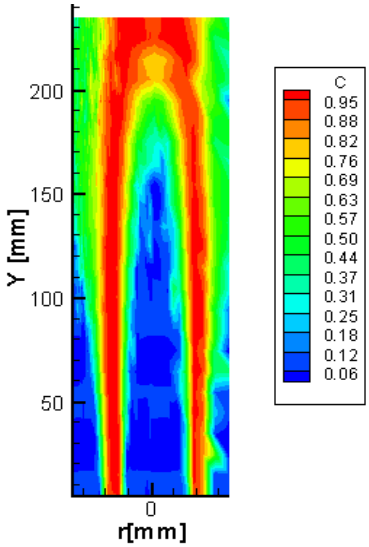

Fig. 10. Contour plot of the mean progress variable <c> (G0.6)

They were interested in the flames of hydrocarbons for various conditions of turbulence. They have shown the increase of the turbulent thickness as a function of the equivalence ratio, as we go away from the stabilization area

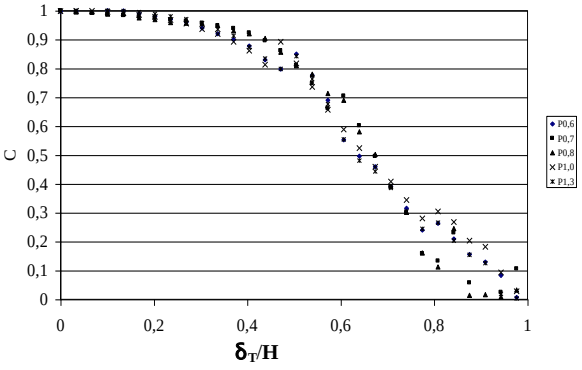

Fig. 11. Profiles normalization of the progress variable at Y/D=0.83, using LST techniques.

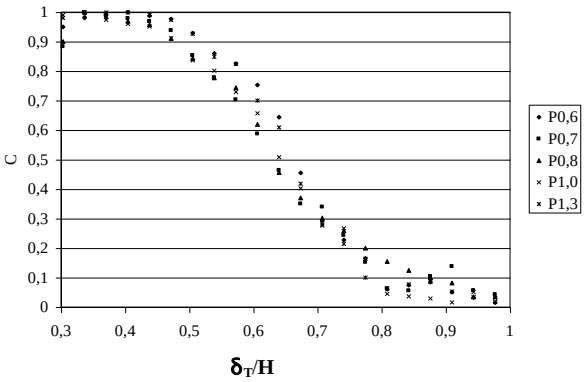

Fig. 12. Profiles normalization of the progress variable at Y/D=0.83, using FCWT techniques

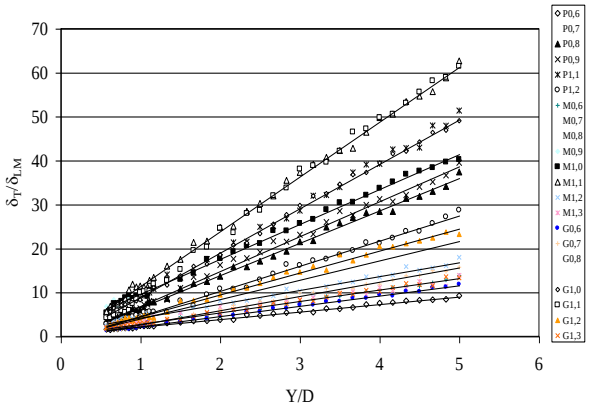

Fig. 13. Flame brush thickness of turbulent flame normalized by the visible laminar thickness and burner diameter (P,M and G grids , and for a range of the equivalence ratio of Ø=0,6 ÷1,3),using LST techniques.

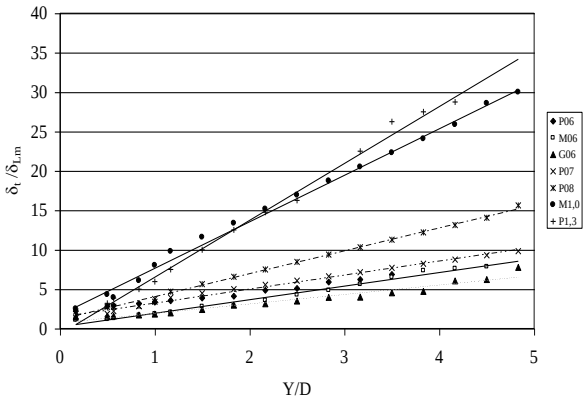

Fig. 14. Thickness of turbulent flame normalized by the visible laminar thickness and burner diameter (P,M and G grids , and for a range of the equivalence ratio of Ø=0,6 ÷1,3),using FCWT techniques.

Further analysis of figure fig. 14, and in order to increase the legibility and the comprehension of δ_T profiles, the latter normalized by the thickness of laminar flame visible δ_{Lm} and the axial distance with the top of the burner by the internal diameter of this one. Jarosinsky [1984] showed experimentaly that for the flames of methane-air this thickness is roughly equal to 6 times the thickness of Zeldovich. For the whole of the flames the thickness has an increasing axial evolution, as it was shown by Boukhalfa & al., [1988], Deschamps [1990], Y.C. Chen & al., [1996] and finally Lipatnikov & Chomiak, [2002]. Our results are also in accordance with the predictions of Prassad & al., [1999]. In figure 9, the two groups of flames are observed, they well represented and distinct.

a) A first family, characterized by a small rate of thickening, a high u'/S_L, as well as weak L_{Lu}/δ_L. It is characterized as well by rich or poor flames which move away from stoeichiometry. At the interior of this family, one can also note the existence of two subclasses:

A first subclass, consisted of the flames P0.6, M0.6, G0.6, M0.7, G0.7, M1.2, M1.3, and G1.3, they are characterized by small $\delta_T/L_M = 9 \div 17$ (with Y/D=5), a high u'/S_L, weak L_{Lu}/δ_L compared with the other flames, as well as small Da, on the other hand Ka is much more important. In this subclass, one can notice two categories: flames P0.6, M0.6, G0.6 having Ka close to the unit, Da and a very small S_L while representing a weak rate of thickening. They belong to the flamelets regime with corrugated flamelets. The remaining of the flames to namely M0.7, G0.7, M1.2, M1.3, and G1.3 present the same properties, but belong to the flamelets regime with corrugated flamelets.

A second subclass formed by the flames P1.2, P0.7, G1.2 and G0.8, presenting $\delta_T/\delta_{TLM} = 22 \div 29$ (with Y/D=5), a large u'/SL, weak L_{Lu}/δ_L compared with that of the other flames, as well as small Da, on the other hand an important Karlovitz number. All these evolutions belong in general to the family of the corrugated flamelets or very close to them.

b) A second family of flames showing the strongest rate of thickening, and whose principal characteristic is that they are all stoechiometric or close to that. One can distinguish the existence of three subclasses:

- The first one including the flames G1.1 and M1.1 and representing the rate of the most important thickening and where δ_T/δ_{LM} exceeds the 60 at Y/D=5. It is characterized by a large S_L and Da, weak Ka, a u'/S_L smaller than the unit and presenting of the most important L_{Lu}/δ_L and are very far away from the origin on the X-axis on the combustion diagram. All these flames are in the wrinkled flamelet regime.
- The second one represented by the flames P1.1 and G1.0 presenting a δ_T/δ_{LM} of 50 (at Y/D=5) and are close a their characteristics to the 1st subclass, and is different only by a L_{Lu}/δ_L wich is slightly smaller.
- The third subclass represented by the flames M1.0, M0.8, P0.9 and P0.8 having $\delta_T/\delta_{LM}= 36 \div 42$, it is characterize (compared to the two previous

subclasses) by a reduction in S_L, Da and L_{Lu}/δ_L, and an increase in u'/S_L and the number of Ka. This subclass is located as a majority in the flamelet regime with corrugated flames. In figure 10, we notice for these distributions which represent the evolutions of turbulent thickness as a function of the equivalence ratio, and for various heights normalized by the burner diameter, that for the poorest flames being at the burner base, the thickness takes relatively smallest values, which increases as one progresses in height and equivalence ratio to reach a maximum value around the stoechiometry, for then approaching a reduction ending with Ø=1.3 giving thicknesses comparable to those obtained for the poor flames.

One obtains practically a factor of 2.33 between the thickness with Ø=0.6 and Ø=1.1 and 2.9 between Ø=1.1 and Ø=1.3, however one can notice a tightening rich side and which end in a slight expansion in the poor flames. Gagnepain, [1998] and Pave, [2002] made the same observations (for restricted values of equivalence ratio), only the factor between the thicknesses was different which can be explained by space differences like in the flames parameters. The behavior of δ_T as a function of the richness is in a relation with the evolutions the of laminar flame speed S_L. A similar behavior was also noticed by Lipatnikov & Chomiak [2002]. The predictions of L.P.H. of Goey [2005] are in a good agreement concord with our experimental results until a richness of 1.1, beyond this value, the theoretical and our experimental results diverge

In order to observe the intensity influence of the axial fluctuation on turbulent flames structure, we represent the thickness results of the turbulent flame front normalized by the visible laminar thickness.

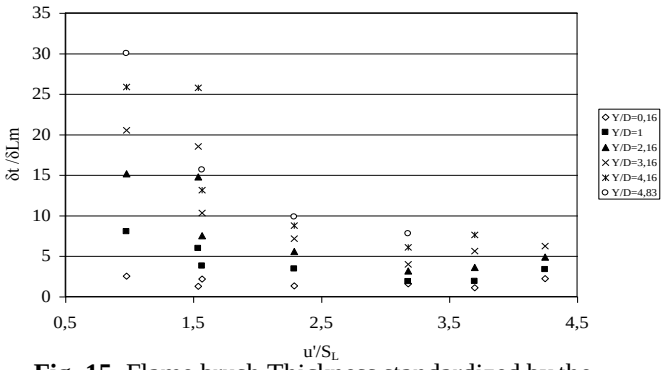

Fig. 15. Flame brush Thickness standardized by the laminar thickness visible according to the number of u'/S_L using LST techniques.

We characterize the turbulence intensity by the known size of the axial fluctuations u' (figure 11), which we standardize by the laminar burning velocity S_L.

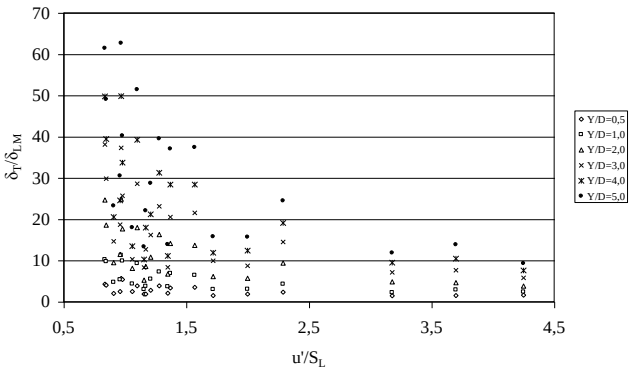

Fig. 16. Flame brush Thickness standardized by the laminar thickness visible according to the number of u'/S_L and for various heights, using FCWT techniques.

Several clear tendencies become apparent in the variation range of Y/D, u' and u'/S_L considered here: we note that the thickness of flame increases when we progresses in the flame and decreases as u'/S_L increases, the intensity of turbulence tends to correlate with the increase in the flame brush. For moderated u'/S_L, the role of flame propagation seems being of great importance, and the effects of the properties of the mixtures on the development of turbulent thickness are real. This suggests that the mechanism of production of turbulence seems to be associated to the properties of the folded flames structures. A similar behavior has been noticed by Buschmann & al., [1996], and is confirmed by the predictions of L.P.H. of Goey & al., [2005] (relative to instantaneous thicknesses). The three modes of combustion are clearly identified:

- u' /SL=0÷1, wrinkled flamelet regime, characterized by thicknesses of important standardized flames,
- u'/S_L=1÷3 corrugated flamelet regime represented by δ_T/δ_{LM} in decrease compared to previously,
- u' /SL=3÷4.5, corrugated flamelet regime close to the Klimov-Williams criterion where δ_T/δ_{LM} are much smaller. In addition, these growths have very close slopes and gradients.

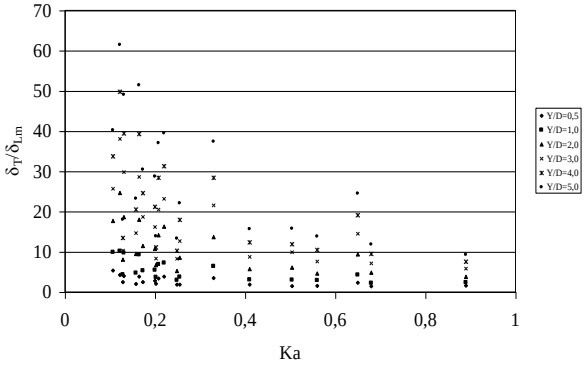

Fig. 17. Flame brush Thickness normalized by the laminar thickness as a function of Karlovitz number for various heights of flame, using LST technique.

These curves integrate the variation effect of the integral scale of a grid into an other of Karlovitz number for various heights of flame, using LST techniques. On figure 12 representing the evolutions δ_T/δ_{LM} as a function of Karlovitz number, we can remark at the exit of the burner, the values of the normalized thickness presents an evolution in plate, for arbitrary values Ka. While progressing in the flame, we can note an increase of the normalized thickness, but decreasing function of Ka.

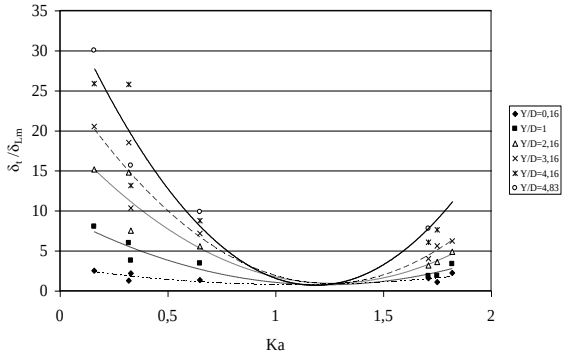

Fig. 18. Flame brush Thickness normalized by the laminar thickness as a function of Karlovitz number for various heights of flame, using FCWT technique.

As on the previous figures (9 and 11), the three modes of flames are quite distinct and clearly identified namely for Ka=0÷0.2 we are in the wrinkled flamelet regime, Ka=0.2÷1 represents the corrugated flamelet regime, Ka=1÷2 indicates a thin reaction zones.

The resulted evolutions from the work of A.Buschmann & al., [1996], as well as the theoretical analysis of L.P.H of Goey & al., [2005] on instantaneous thicknesses are in agreement with our results.

Figure 13, represents the evolution turbulent thickness normalized as a function of the Damkôhler number, for several heights normalized by the burner diameter. We can notice that first of all that for all the heights the general tendency indicates an increase of the normalized thickness according to Da. Very weak at the base of burner (Y/D=0.5), it increases when one progresses in the flame to reach a maximum with Y/D=5. As Boukhalfa & al., noted. [1988] the evolutions of δ_T/δ_{LM} increase abruptly to reach their first maximum with Da=12. This value is considered as critical and boundary value between the mode of the folded and the thickened flames. It decrease first once until Da=18 then goes up until a second maximum around Da=30, for finally going down again until Da=42. We observe, however that Da=42 is a limiting value, characterized by an abrupt reduction in δ_T/δ_{LM} what ever is the height of flame and which corresponds to transition of the wrinkled flamelet regime to corrugated flamelet regime. Exceeding this characteristic point the shapes of the curves take again the evolutions and the slopes which they had before. (Da=15 for Boukhalfa & al., [1988]).

N°	$\bar{U}$ [m/s]	u' [m/s]	u'/U %	L_{Lu} [mm]	S_L [cm/s]	u'/S_L	δ_L [mm]	a.10^{-6} [m^2/s]	ReT	τ_{ad}	t_c [ms]	Φ	L_{Lu}/δ_L	Da	Ka
P0.6	5.75	0.425	7.5	6.0	10	4.25	0.259	21.4	170	4.69	1.87	0.6	23.16	5	0.86
P0.7	5.75	0.425	7.5	6.0	18.5	2.29	0.216	21.4	170	5.20	0.94	0.7	27.77	12	0.65
P0.8	5.75	0.425	7.5	6.0	27	1.57	0.173	21.4	170	5.61	0.58	0.8	34.28	22	0.33
P0.9	5.75	0.425	7.5	6.0	33	1.28	0.144	21.4	170	5.99	0.39	0.9	41.66	32	0.22
P1.0	5.75	0.425	7.5	6.0	37.5	1.13	0.122	21.4	170	6.38	0.27	1.0	49.18	43	0.17
P1.1	5.75	0.425	7.5	6.0	38	1.1	0.110	21.4	170	6.19	0.39	1.1	54.54	50	0.16
P1.2	5.75	0.425	7.5	6.0	35	1.21	0.144	21.4	170	6.00	0.58	1.2	41.66	34	0.21
P1.3	5.75	0.425	7.5	6.0	27.5	1.54	0.173	21.4	170	5.81	0.94	1.3	34.68	22	0.32
M0.6	5.68	0.37	6.4	6.5	10	3.7	0.259	21.4	160	4.69	1.87	0.6	25.00	6.78	1.75
M0.7	5.68	0.37	6.4	6.5	18.5	2.0	0.216	21.4	160	5.20	0.94	0.7	30.00	15.04	0.63
M0.8	5.68	0.37	6.4	6.5	27	1.37	0.173	21.4	160	5.61	0.58	0.8	37.57	27.42	0.32
M0.9	5.68	0.37	6.4	6.5	33	1.12	0.144	21.4	160	5.99	0.39	0.9	45.13	40.26	0.21
M1.0	5.68	0.37	6.4	6.5	37.5	0.98	0.122	21.4	160	6.38	0.27	1.0	53.27	54.00	0.16
M1.1	5.68	0.37	6.4	6.5	38	0.97	0.110	21.4	160	6.19	0.39	1.1	59.09	60.68	0.15
M1.2	5.68	0.37	6.4	6.5	35	1.06	0.144	21.4	160	6.00	0.58	1.2	45.13	42.70	0.20
M1.3	5.68	0.37	6.4	6.5	27.5	1.35	0.173	21.4	160	5.81	0.94	1.3	37.57	27.90	0.31
G0.6	5.28	0.318	6.0	6.8	10	3.180	0.259	21.4	144	4.69	1.87	0.6	26.25	8.25	0.54
G0.7	5.28	0.318	6.0	6.8	18.5	1.720	0.216	21.4	144	5.20	0.94	0.7	31.48	18.31	0.29
G0.8	5.28	0.318	6.0	6.8	27	1.170	0.173	21.4	144	5.61	0.58	0.8	39.30	33.37	0.31
G0.9	5.28	0.318	6.0	6.8	33	0.960	0.144	21.4	144	5.99	0.39	0.9	47.22	49.00	0.21
G1.0	5.28	0.318	6.0	6.8	37.5	0.848	0.122	21.4	144	6.38	0.27	1.0	55.73	65.72	0.16
G1.1	5.28	0.318	6.0	6.8	38	0.836	0.110	21.4	144	6.19	0.39	1.1	61.82	74	0.15
G1.2	5.28	0.318	6.0	6.8	35	0.908	0.144	21.4	144	6.00	0.58	1.2	47.22	52	0.17
G1.3	5.28	0.318	6.0	6.8	27.5	1.156	0.173	21.4	144	5.81	0.94	1.3	55.73	34	0.31

Table1: Experimental conditions

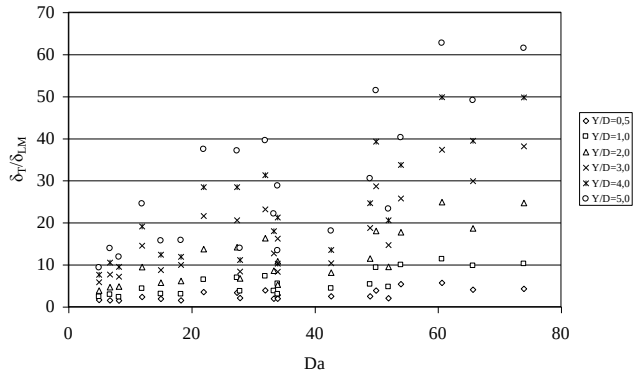

Fig. 19. Comparison of the turbulent Flame brush thickness normalized by the laminar thickness according to the Damkôhler number, using LST technique.

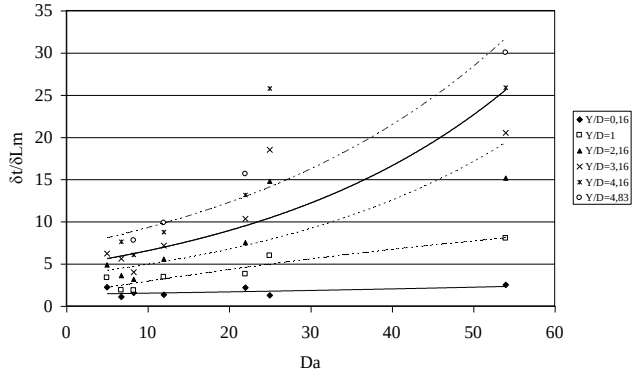

Fig. 20. Comparison of the turbulent Flame brush thickness front normalized by the laminar thickness according to the Damkôhler number, using FCWT technique.

We compared the results of two measurement techniques. This is a part of the plane laser tomography (LST), and thermometry digitally compensated fine wire (FCWT), whose results were presented separately in the previous chapters. The results of measurements of the turbulent flame thickness were normalized by the thickness of laminar flame apparent δT / δLM, and the axial component by the diameter of the burner. Figures III.75, III.76, III.77, III.78, III.79 and III.80 represent a comparison between the results of tomography and thermometry, flames P0.6, M0.6, G0. 6, P0.7, P0.8 and M1.0. The other fires have been compared by lack of thermometric results. We note that a point of view both qualitatively and quantitatively our experimental results from both techniques are generally in good agreement. They are very good at the base of the burner to Y/D=2, then the values differ in some cases, mainly because of sharp fluctuations due to instabilities, which describe the dynamics of instantaneous flame fronts in the "flame brush and in the plume. The curves have the same effect gaits, similar slopes and sometimes overlap exactly

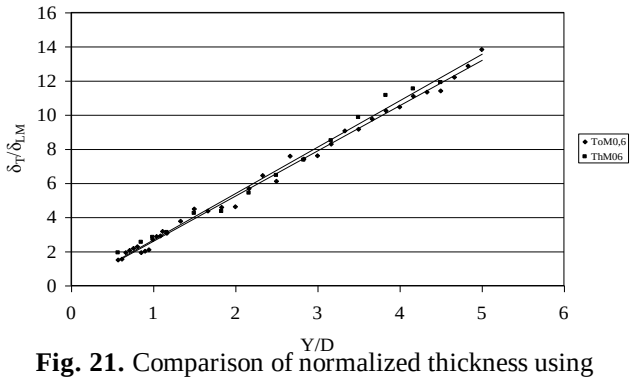

Fig. 21. Comparison of normalized thickness using LST and FCWT for flame ***M0,6***

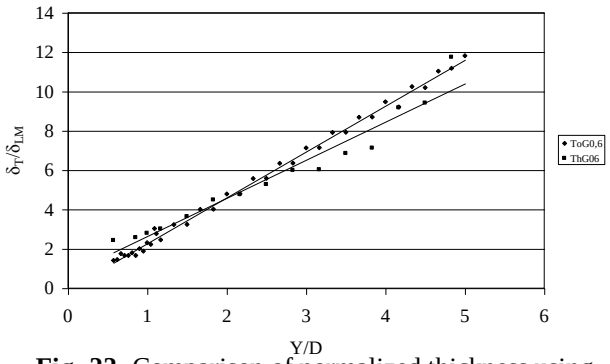

Fig. 22. Comparison of normalized thickness using LST and FCWT for flame ***M.07***

Conclusion

The experimental study of the turbulent flames is a way to confirm the existence various types flame structures. In the light of all the preceding results, representing an analysis of flame brush thickness normalized in different way (δ_{LM} and L_{LU}) according to various parameters (Y, Y/D, Y/H, u'/U, u'/S_L, Da, and Ka), we can clearly note that:

- the normalized thickness variations are weak at the exit of the burner, and take importance more and more as one progresses in the flame,
- mixture richness has great importance on the development of the flame scalar structure, and the evolution of the turbulent thickness is Gaussian of which the maximum is located around the stoechiometry,
- turbulence has as an effect to increase the turbulent thickness,
- analysis based on the adimensional numbers of Damkôhler, Karlovitz and u' /S_L allows to define the various modes of flame starting from the normalized turbulent thicknesses. The various modes of flame are as follows:

a) wrinklet flamelet regime, characterized by a great normalized thicknesses, a u'/S_L<1, a Da=49÷74 and a Ka= 0.15÷0.2,

b) corrugated flamelets regime represented by a less important normalized thicknesses, a u'/S_L=1÷2.3, a Da=12÷49 and a Ka= 0.2÷0.65,

c) Last regime is thin reaction where we found a loss normalized thicknesses, a u'/S_L=3÷4.25, a Da=5÷12 and a Ka= 1.72÷1.82.

Acknowledgments
The author gratefully acknowledge technical support by the Coria of Rouen (France). The authors also thank A.M. BOUKHALFA (Coria Rouen) for the stimulating discussions, B. RENOU (Combustion Diagnostics Group Coria Rouen) for their help in setting up and operating the laser system, and B. TAUPIN, O. DESGARDIN, G. MARTINS and C. LACOUR (Coria Rouen) for his help in developing part of the image post-processing routine.

References

[1] A. Boukhalfa, I. Gokalp I., Comb. Flame 73 (1988) 75-87.
[2] A. Boukhalfa, Ph.D. Thesis. Université d'Orléans, 1988.
[3] M.S. Boulahlib, B. Renou, A. Boukhalfa, Z. Nemouchi, Sci & Tech, 22B (2004) 67-78.
[4] M.S. Boulahlib, B. Renou, I. Amara, A. Boukhalfa in Proceed of Advanced Mathematical and Computing Tools in Metrlogy and Testing AMCTM2008 23-25 June 2008 ENS Paris, France.
[5] L. Boyer, Comb. Flame 39 (1980) 321-323.
[6] F. Buschmann, F. Dinkelacker, T. Schäfer, M. Schäfer, J. Wolfrum, Proc. Comb. Inst. 26 (1996) 437-443.
[7] Y.C. Chen Y.C., M.S. Mansour, Proc. Comb. Inst. 27 (1998) 437-443 811-818**.**
[8] Y.C. Chen, R.W. Bilger, Proc. Comb. Inst. 30 (2004) 801-808.
[9] G. Comte-Bellot, "Turbulence" Cours de mécanique des fluides, Ecole Centrale de Lyon, 1982, France.
[10] L.P.H De Goey., T. Plessing, R.T.E. Hermanns N. Peters, Proc. Comb. Inst. 30 (2005) 859-866.
[11] S.G. Filatyev, J.F. Driscoll, C.D. Carter, J.M. Donbar, Comb. Flame 141 (2005) 1-21.
[12] L. Gagnepain, Ph.D Thesis, Université d'Orléans 1998 France.
[13] P. Goix, Ph.D Thesis, Université de Rouen, 1987 France.
[14] P. Griebel., P. Siewert, P. Jansohn, Proc. Comb. Inst. 31 (2007) 3083-3090.
[15] J. Jarosinski, Comb. Flame 56 (1984) 337-342.
[16] A.N. Lipatnikov, J. Chomiak, Pro En Comb Science 28 (2002) 1-74.
[17] A.N. Lipatnikov, and J. Chomiak, Proc. Comb. Inst. 30 (2005) 843-850.
[18] M. Namazian, R.W. Sheffer, J. Kelly, Comb Flame 74 (1988) 147-160.
[19] D. Pavé Ph.D Thesis. Université d'Orléans, 2002 France.
[20] N. Peters, Proc. Comb. Inst. 7 (1987) 461-468.
[21] N. Peters, B Rogg, 15 Lect. Not. In Physics, Springer-Verlag, Berlin, 1993.
[22] N. Peters, "Turbulent combustion" Cambridge University Press, Cambridge, 2000.
[23] T. Poinsot, D. Veynante, S. Candel J. Fluid Mech., 228 (1991) 561-606.
[24] B. Renou, A. Boukhalfa, D. Puechberty, M. Mouqualid, M. Trinité, Combustion, N°1 vol. 2 (2000) 85-112.
[25] E. Rouland, Ph.D Thesis, Université de Rouen, (1994) France.
[26] R. Said, Ph.D. Thesis, Université de Rouen, (1989) France.
[27] A. Soika, F. Dinkelacker, A. Leipertz**,** Proc. Comb. Inst. 27 (1998) 785-792.
[28] A. Soika, F. Dinkelacker, A. Leipertz Proc. Jo. meet. Brit., Ger. and Frenc. Sect. of The Combustion Institute, Nancy France, pp. 463-465, 1999.
[29] D. Spalding, Proc. Comb. Inst. 13 (1971) 649-657.